2008 IEEE International Conference on
Robotics and Automation
Pasadena, CA, USA, May 19-23, 2008

Demonstrating the Safety and Performance of a Velocity Sourced Series Elastic Actuator

Gordon Wyeth, *Member, IEEE*

***Abstract*—Actuators with deliberately added compliant elements in the transmission system are often described as improving the safety of the actuator at the detriment of the performance. We show that our variant of the Series Elastic Actuator topology, the Velocity Sourced Series Elastic Actuator, has well defined performance characteristics that make for improvements in safety *and* performance over conventional high impedance actuators. The improvement in performance was principally achieved by having tight velocity control of the DC motor that acts as the mechanical power source for the actuator. Results for performance are given for point to point transition times, while results for safety are based on empirical assessment of the Head Injury Criterion during collisions.**

I. Introduction

The new field of human-centered robotics addresses the many challenges in creating close interactions between humans and robots, including direct contact between robots and humans. Current standards for robot safety prohibit such contact, specifying failsafe robot enclosures that keep humans completely out of the robot's workspace at all times, and removing the possibility of direct interaction. The issue of robot safety is being addressed by a range of strategies that operate to either prevent collisions or to minimize the harm caused by collisions.

Many researchers are investigating the use of compliance in the transmission systems of robot actuators as a means of reducing forces during an accidental impact ([1],[2],[3],[4]). A compliant transmission system coupled with light weight mechanical design reduces the mechanical impedance of the manipulator. Most robots use high impedance actuators typical of industrial robot arms. When a high impedance robot collides with an obstacle, the forces are large and rise quickly, maximizing the likelihood of injury.

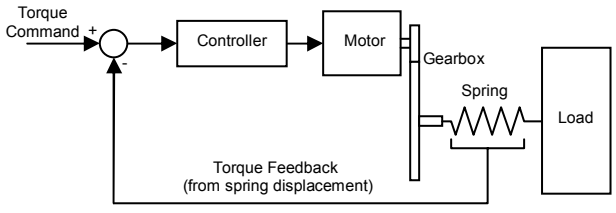

Figure 1: Series Elastic Actuator topology.

Manuscript received September 14, 2007.

Gordon Wyeth is with the School of Information Technology and Electrical Engineering, University of Queensland, Brisbane, 4072, Australia (phone: +61 7 3365 3770; fax: +61 7 3365 4999; e-mail: wyeth@itee.uq.edu.au).

To achieve a low impedance design it is imperative to decouple the high moment of inertia of the motor seen through the gearbox which can create a high impact load. The Series Elastic Actuator (SEA) deliberately introduces compliance via a spring between the motor-gearbox and the load, and so has intrinsic low impedance. However, it is widely held that the SEA has bandwidth limited to about one-third of the fundamental frequency, and that attenuation of flexible mode oscillations can be difficult to achieve [5].

This paper shows that it is possible to produce high performance from an SEA, well beyond one-third of the fundamental frequency, while retaining the inherent safety given by the actuator's low effective inertia and stiffness. The improvement in performance is principally achieved by having tight velocity control of the DC motor that acts as the mechanical power source for the actuator. This variant of the SEA, the Velocity Sourced SEA (VS-SEA), has well defined performance characteristics that help to define trajectories that are both achievable and safe.

The paper reviews the principles of the Velocity Sourced SEA, and than gives a description of a prototype device and its controller. The safety of the VS-SEA is evaluated by a series of quantitative measurements of the Head Injury Criteria (HIC) [6], a standard used in automotive safety. Performance is compared with a high impedance actuator system based on the same DC motor and gearbox for point to point time trials conducted within the safe speed limits of the respective devices.

II. Previous SEA Studies

The control and implementation of Series Elastic Actuators have been approached from a number of perspectives. In [7], the concept is first introduced in the form of an electric motor in series with a spring. The spring in this model was a beam with a cross-shaped cross section. Deflection in the beam was measured using strain gauges. The motor was controlled using current control as the input to the motor, making the motor an effective torque source. The compensation scheme used both feedback from the strain gauges, and feedforward from the desired torque input to calculate a desired current for the motor. While the implementation demonstrated many of the desirable characteristics of a Series Elastic Actuator, there were a number of undesirable characteristics in the design. Backlash in the gearbox introduced some undesirable and unpredictable resonances in the closed loop response, and friction effects limited the effectiveness in providing large

force bandwidth. In [8], the author notes potential for improvement in the electronic design of the system.

The SEA was revisited in detail in [9] again with the supposition that the motor is to be controlled as a torque source. The effects of friction and backlash are better quantified, and some guidelines for spring selection are introduced. The actuators themselves formed the basis of the acuators for sale through Yobotics. Later work [2] however describes similar problems to those seen by Williamson.

III. Velocity Sourced SEA

In this paper, we change the paradigm for SEA design by treating the motor as a velocity source rather than as a torque source. This idea is suggested in [9]. The reason that this idea becomes attractive is that a tight velocity control of the motor can overcome some of the undesirable effects of the motor and the gearbox and provide a consistent platform for the outer SEA controller.

The principle of a velocity controlled SEA is shown in Figure 2. The motor has velocity feedback from an encoder that forms a tight loop for controlling the motor and gearbox. The velocity controller is tuned with no load attached, based on the assumption that the spring decouples any high-frequency torque disturbances on the SEA output, and that a well tuned velocity controller should be able to deal with low-frequency torque disturbances. With this tight velocity control loop in place, the motor can be treated as an effective velocity source, simplifying the design of the SEA controller for the outer torque loop.

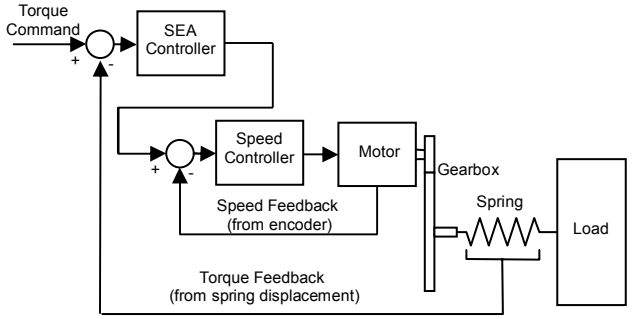

Figure 2: The inner velocity loop in the velocity source SEA helps to overcome problems with non-linearities and stiction.

A. Dynamics of a Velocity Sourced SEA

With the motor acting as a velocity source, the equations of motion associated with the SEA can be written. The spring deflection θ_s is a function of the motor speed ω_m and the position of the load θ_L:

$$\theta_s = \frac{\omega_m}{s} - \theta_L \tag{1}$$

Assuming that the load has inertial properties, J_L, and is being controlled only by the actuator, that is, that there are no other torque sources affecting the load, then the position of the load is determined from the output torque applied to the load T_L:

$$\theta_L = T_L \frac{1}{J_L s^2} \tag{2}$$

But the torque applied to the load T_L is due solely to the deflection of the spring θ_s by:

$$T_L = K_s \theta_s \tag{3}$$

By combining (1), (2) and (3) we find the open loop transfer function from motor velocity to SEA output torque is given by:

$$\frac{T_L}{\omega_m} = \frac{K_s s}{s^2 + \frac{K_s}{J_L}} \tag{4}$$

where T_L is the output torque applied to the load, ω_m is the speed of the motor, J_L is the inertia of the load and K_s is the spring constant. If the velocity source is a DC motor in a closed loop with PI compensation, the closed loop motor transfer function will have the form:

$$\frac{\omega_m}{\omega_d} = \frac{B}{s^2 + As + B} \tag{5}$$

where A and B are some constants derived from the choice of zero placement and gain in the PI controller to achieve fast rise time and little overshoot. These poles will be much faster than the imaginary poles of the velocity to torque transfer function.

B. Choosing a Control Strategy

Placing the motor and series elastic element transfer function in series gives the open loop transfer function that must be compensated by the SEA controller:

$$\frac{T_L}{\omega_d} = \frac{BK_s s}{(s^2 + As + B)(s^2 + \frac{K_s}{J_L})} \tag{6}$$

To create a system that will be of Type 1 with respect to a torque input (no steady state error for a constant torque) the compensator must have two poles at the origin. Choosing two low frequency, complex zeroes tends to attract the resonant poles of the SEA to those zeroes, cancelling the resonance. This compensator has the form:

$$\frac{\omega_d}{T_e} = \frac{K_{SEA}(s^2 + Cs + D)}{s^2} \tag{6}$$

where C and D are chosen to attract the resonant poles under feedback, and the gain K_{SEA} can be determined from a root locus plot. In the following section, we will demonstrate a case study of the design of a controller after describing the implementation of our VS-SEA.

IV. Implementation

We have built a prototype VS-SEA to test the concept's suitability for use in human-robot interaction applications. The following section outlines the design of the prototype including the hardware and the controller. The effects of saturation are addressed, and the system for trajectory generation explained. The high impedance reference system used for comparison is described.

A. Hardware Design

The design treats the elastic element as a modular

component that might be used with a range of motor systems, as are other transmission elements such as gearboxes. The elastic element (illustrated in Figure 3) is 120 mm in diameter, and 98.5 mm in length, comprising a body 36 mm long, with 25 mm of output shaft and 37.5 mm of input shaft. With four springs, the element provides a rotational spring constant of 138 Nm/rad, although the design can use less springs or accommodate a range of spring sizes. The springs are always in compression and remain linear in their behavior.

The deflection sensor is a critical element in the design, as noise or quantization in the angle measurement impacts system performance dramatically. We have employed a Philips KMZ-41 Magnetic Field Sensor in a 150 kA/m field, achieving an absolute position measurement with 0.01° of resolution.

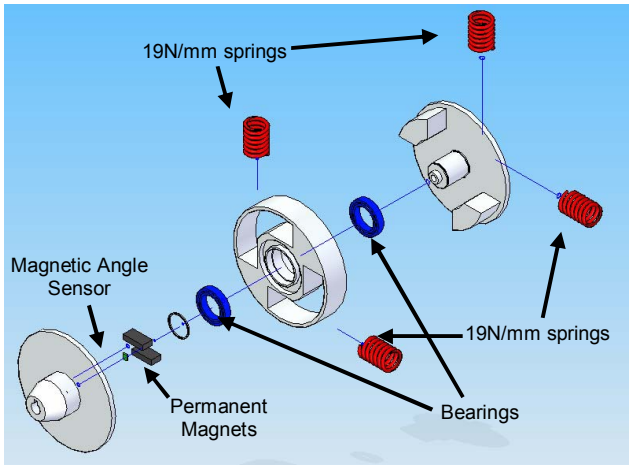

Figure 3: Exploded view of the Series Elastic element used in the VS-SEA.

The elastic element is actuated by a Maxon RE35 90W 42V motor with an integrated GP42C 156:1 planetary gear head and a HED-5540 500CPT encoder. The motor / gear head / encoder has the relevant characteristics listed in Table 1 below.

For these experiments, the element drives a 5 kg link with length 0.6 m and a moment about the actuator drive axis of 0.6 kg/m^2. The dimensions are typical of the combined properties from the shoulder of an arm used in human-robot interactions. It is significantly heavier than other studies [4], [1], but is perhaps truer to the achievable mass if the arm is to be equipped with a dexterous gripper.

Control is performed by a custom motor drive board with a 25 MHz 32 bit microcontroller, with sensing and power electronics. The motor drives are rated to 60V at 5A, but can provide up to 20 A peak. Power is drawn from laboratory supplies using a 42 V bus. The control system is implemented as a discrete time digital system, based on the ensuing continuous time design. The sample rate for the discrete system is 3.6 kHz.

TABLE I
PROPERTIES OF MOTOR USED TO DRIVE THE VS-SEA.

Property	Value
Nominal voltage	42 V
Terminal resistance	2.07 Ω
Terminal inductance	0.62 mH
Torque constant	0.0525 Nm/A
Back EMF constant	0.0528 Vs/rad
Max speed	859 rad/s
Max continuous torque	0.115 Nm
Rotor inertia	6.96×10^{-6} kg.m^2
Reflected gear head inertia	0.91×10^{-6} kg.m^2
Gear ratio	156:1
Coulomb friction (at output)	10 mNm
Coefficient of viscous friction	0.7

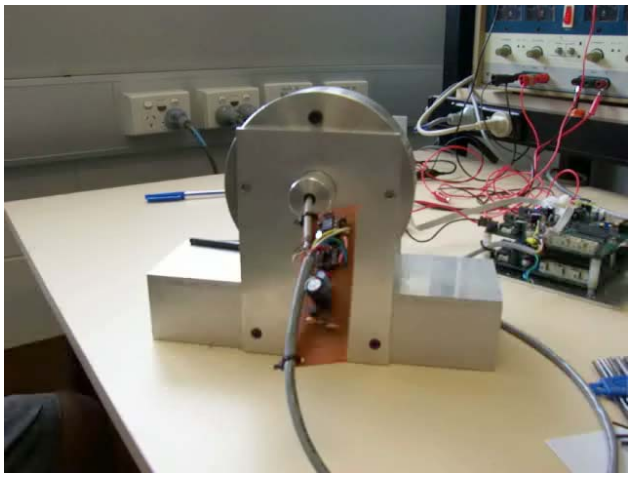

Figure 4: The velocity sourced SEA in its test rig. The prototyping board is a preamplifier for the magnetic field sensor.

B. *Controller Design*

With the prototype system configured as described above the system has open loop transfer function in the form of equation (6) with the following values:

$$\frac{T_L}{\omega_d} = \frac{1780^2.138/156.s}{(s^2+3130s+1780^2)(s^2+230)} \qquad (7)$$

Using the control strategy described in section III B we tried a number of complex zero positions near the resonant poles. Using a root locus plot we chose zeroes at -10 ± 26.5j and a gain of 300 giving the compensator transfer function:

$$\frac{\omega_d}{T_e} = \frac{300(s^2+20s+800)}{s^2} \qquad (8)$$

The final closed loop transfer function for torque command is:

$$\frac{T_L}{T_d} = \frac{8.4\times10^8(s^2+20s+800)}{(s+374)(s^2+19s+862)(s^2+2740s+1450^2)} \qquad (9)$$

Note that, as observed by Robinson [9], the transfer function can be independent of the spring stiffness. Any change in spring stiffness can be offset by an equal and opposite change in the controller gain. Note also that the bandwidth of the linear system has significantly exceeded the resonance of the compliant system, but it is important to verify that that is the case with the non-linearities – most

notably motor saturation – in the implemented system.

C. Effects of Saturation

In considering the effects of saturation on the implemented system, it is important to think of the motor as a velocity source with the principle role of controlling the length of the spring between motor and load that in turn controls torque (1). Considering just the fast-acting movement associated with the motor and spring rather than the steady state speed of the load, one can write:

$$\omega_m \cong \frac{\dot{T}_L}{K_s} = \frac{J_L}{K_s}\ddot{\omega}_L \tag{10}$$

That is, the speed of the motor defines the rate of change of torque which in turn defines the jerk of the load. The maximum speed of the motor is the key saturation effect that defines the performance of the VS-SEA.

The implications from this observation are twofold. Firstly, the VS-SEA can not source a step change in torque, but, given a tight velocity loop around the motor with fast rise time, will slew torque at a near constant rate of change. For a fixed load, this implies a limit to the jerk of the trajectory of the load. Secondly, the jerk value is readily discernable from the VS-SEA parameters, and if the load trajectory is planned with that limited jerk capability in mind then the controller will continue to operate in a linear and predictable fashion.

D. Trajectory Generation

The trajectory generation system takes arbitrary velocity command streams and converts them to torque commands that respect the torque limits of the motor imposed by thermal constraints and the torque slew limits imposed by the limits to motor speed (as described above).

$$\tau_{ff} = f(\omega_{DL}, \dot{\omega}_{MAX}, \ddot{\omega}_{MAX}) \tag{11}$$

The computed torque is based on estimates of load inertia and losses. To prevent a build-up of error from errors in estimates or noise, the torque profile is supplemented by feedback control from a spring-damper virtual model. The velocity profile is integrated to create a desired angle θ_D for the joint, which is compared to the link angle θ_L derived by summing the angle of the motor θ_M (from the encoder) with the angle of the spring θ_S (from the torque sensor). The controller has a spring constant K_s of 20 N / rad and a damper constant K_d of 1 Ns / rad. The torque command to theVS-SEA is calculated by:

$$\begin{aligned} \theta_{err} &= \theta_D - (\theta_M + \theta_S) \\ \tau &= K_d\theta_{err} + K_S\dot{\theta}_{err} + \tau_{ff} \end{aligned} \tag{12}$$

E. High-Impedance Reference System

For the purposes of comparative study, a high impedance actuator system was implemented based on the same hardware as the Velocity Sourced SEA. This actuator has the SEA element removed, allowing the motor to directly drive the link. With the speed controller implemented with well tuned PI compensation (P = 100, I = 5000) the closed loop transfer function is:

$$\frac{\omega_m(s)}{\omega_d(s)} = \frac{1.69\times10^6(s+50)}{(s+2664)(s+624)(s+50.8)} \tag{11}$$

Trajectories are generated by supplying a stream of desired velocities at the system sampling rate (3.6 kHz). The nature of the trajectories used is described in the relevant experiments.

V. Experiment Setup

A. Establishing Safe Limits

Safety is assessed using the Head Injury Criterion (HIC) [6], a method for assessing the injury probability based on the acceleration of the head during an impact. The HIC is defined as:

$$\mathrm{HIC} = \max_{t_2-t_1\le\Delta}\left\{\left[\frac{1}{t_2-t_1}\int_{t_1}^{t_2} a(t)dt\right]^{2.5}(t_2-t_1)\right\} \tag{12}$$

where $a(t)$ is the linear acceleration at centre of the head (notionally the brain) and Δ is a maximum duration set to limit the time extent over which an impact can be considered (set to 15 ms). An HIC limit of 100 has been variously quoted as a suitable limit for interactive robots [5], [1].

The head is modeled as a 5 kg spherical mass on a low friction surface with a firm, elastic covering. Collisions occur normal to the surface of the head and parallel to the low friction surface. The covering has a spring constant of ~10 kN/m and damping of ~100 Ns/rad. The 5 kg link strikes the head at 0.5 m along the link's length. Tests were made over a range of velocities and compliances

B. Establishing Performance

Performance is established by using the trajectory generator to execute 22.5°, 45°, 90° and 180° rotations of the link starting and stopping at rest. The maximum speed of rotation is set to safe limits for the given system compliance based on results from HIC testing. The maximum acceleration ω_{MAX} is fixed at 21 rad/s^2 which corresponds to the maximum torque ability of the motor for the fixed load. The jerk of the trajectory is set to suit the compliance between the motor and gearbox based on:

$$\ddot{\omega}_{MAX} = \beta\frac{K_s\omega_{LIMIT}}{J_L} \tag{13}$$

where β is a discounting factor that allows for motor speed to be used driving the load, and ω_{LIMIT} is the maximum speed of the motor at the gearbox output shaft (5.5 rad/s). In the following tests β = 25%.

VI. Results

A. Safety versus Speed

The safety was assessed for the VS-SEA over a range of collision speeds using the Head Injury Criterion. The Head Injury Criterion was also assessed for the high impedance actuator for the same set of collision speeds. The results in Figure 5 indicate an upper bound on safe speed of 3.3 m/s

for the VS-SEA compared to 2 m/s for the high impedance actuator (based on a limit of HIC of 100).

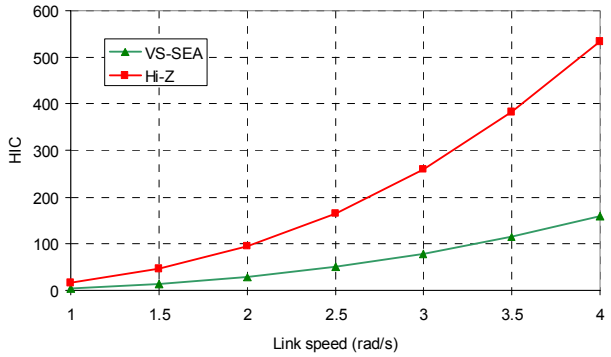

Figure 5: HIC values for a range of link speeds for the VS-SEA and the high impedance (Hi-Z) actuator. An HIC of 100 is generally considered the limit for safe operation of an interactive robot.

B. *Safety versus Compliance*

The HIC was also assessed for a range of spring compliances. The compliance of our VS-SEA design is easily changed by removing springs from elastic element. As outlined in the controller design section, the gain in the controller was adjusted to compensate the change in compliance. With a single spring, the compliance is 34 Nm/rad, representing a four fold decrease in compliance. When the controller gain is increased four-fold to compensate, there is negligible impact of the safety of the SEA as measured by the HIC. This is contrast to the findings of [1], most probably as the spring stiffness is too low to reach the steeper parts of the HIC / stiffness curve.

C. *Performance*

Performance was assessed by executing trajectories over 22.5°, 45°, 90° and 180° using first the VS-SEA and then the high impedance actuator. The VS-SEA trajectories were limited in jerk based on (13) to 316 rad/s^3 (using all four springs). The results are shown in Figure 6. Comparing the velocity profiles of the two actuators for a 90° turn (Figure 7) reveals the expected difference between the two actuators – the VS-SEA has a higher safe top speed, but takes longer to reach that speed – that explains the results of Figure 6. Over short angles, the high impedance actuator performs better, but for angles of greater than 30° the VS-SEA outperforms the stiff actuator. From the results presented here, our prototype VS-SEA could benefit from a stiffer spring allowing higher jerk without impacting the safe speed. The compromise would be a loss of torque resolution from the spring displacement sensor.

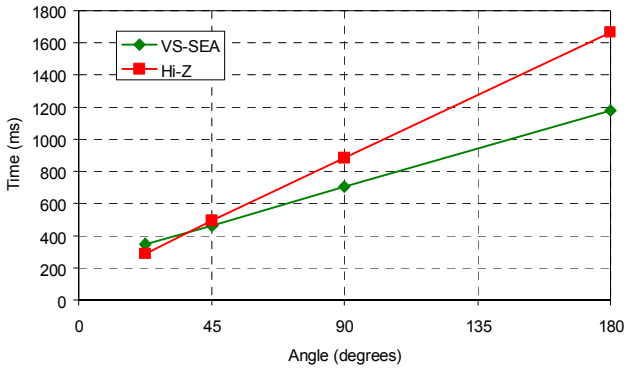

Figure 6: Time to execute a safe movement across a variety of angles for the VS-SEA and the high impedance actuator.

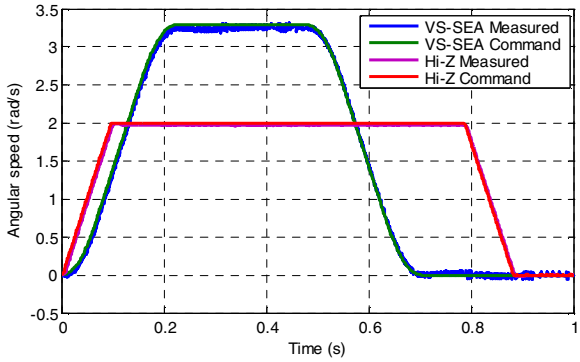

Figure 7: Velocity profiles for the VS-SEA and the high impedance actuator, showing commanded and measured velocity, for a 90° rotation.

The plot in Figure 7 shows the velocity derived from the digitally filtered derivative of the encoder and spring length measurements for the VS-SEA, and the digitally filtered derivative of the encoder for the high impedance actuator. The greater noise in the VS-SEA encoder signal is attributable to the added noise from the derivative of the magnetic sensor. The offset in magnitude in both encoder signals is due to quantization errors in the digital filter.

D. *Energy Consumption*

Some observations on energy usage were made by using high fidelity simulations. The VS-SEA must rapidly add energy to spin up the armature in order to meet jerk demands, and then slow it again when jerk drops to zero. Both operations require current from the bus, and significant energy is wasted both mechanically ($\frac{1}{2}J_a^2\omega$) and electrically (I^2R_a). Table 2 shows the estimated energy usage and armature temperature rise based on simulation results. While it may be possible to capture and re-use the energy in the spinning armature with suitable power electronics, the I^2R losses leading to temperature rise in the armature cannot be overcome when using the velocity source approach. The value of the gains in safe performance should be weighed against the extra energy used.

TABLE II
ENERGY USAGE OVER A 90°TURN

Measure	VS-SEA	High Impedance
Integral of instantaneous electrical power (J)	26	11
Temperature rise in rotor (°K)	2.4	1.1

E. Qualitative Observations

The VS-SEA is generally robust in its behavior, provided that it is driven within its limits. For example, during testing, the VS-SEA was often run with the link removed. With only the output plate as load inertia, the VS-SEA was quite stable while commanded to produce zero torque. Motion could be started or stopped by a light rub of the output plate with the finger. The VS-SEA is similarly stable against stiff loads (the output plate is held still) when torques are commanded.

The VS-SEA does not always behave well when pushed outside its limits in either commanded speed, acceleration or jerk. It may be prudent to use anti-windup on the various integrators in the controllers to get a more graceful degradation in performance when limits are exceeded.

VII. CONCLUSION

The VS-SEA provides enhanced safety over a conventional gear-motor actuator, and improves safe performance times for most operations. By treating the motor that drives the VS-SEA as a velocity source, the compliance in the drive train is seen as a limit in the rate of change of torque. By factoring that limit in the rate of change into trajectory generation, the VS-SEA can produce fast, reliable and safe trajectories for a range of loads. The VS-SEA has all of the side benefits of an SEA also, most notably a low cost torque sensor that facilitates torque based control and other safety benefits such as collision detection. The VS-SEA performance appears comparable to other more mechanically complex devices such as DM^2 [5] and VST [10], although a study with a lighter link mass would be required for a fair comparison. The chief disadvantage of the VS-SEA is that it uses over twice the energy of its high impedance counterpart, which may not be an acceptable tradeoff against the safe performance gains.

ACKNOWLEDGMENT

I would like to thank Dr Geoffrey Walker for his contributions in preparing the electronics for the VS-SEA, and his comments on the project and this paper.

REFERENCES

[1] A. Bicchi and G. Tonietti, "Fast and “Soft-Arm” Tactics: Dealing with the Safety-Performance Tradeoff in Robot Arms Design and Control," *IEEE Robotics & Automation Magazine*, pp. 22-33, 2004.

[2] G. A. Pratt, P. Willisson, C. Bolton, and A. Hofman, "Late Motor Processing in Low-Impedance Robots: Impedance Control of Series Elastic Actuators," presented at Proc of American Control Conference, Boston, MA, 2004.

[3] D. W. Robinson, J. E. Pratt, D. J. Paluska, and G. A. Pratt, "Series Elastic Actuator Development for a Biomimetic Walking Robot," presented at IEEE/ASME Int'l Conf. On Adv. Intelligent Mechatronics, 1999.

[4] M. Zinn, O. Khatib, B. Roth, and J. K. Salisbury, "A New Actuation Approach for Human-friendly Robot Design," *International Journal of Robotics Research*, vol. 23, pp. 379-398, 2004.

[5] M. Zinn, O. Khatib, B. Roth, and J. K. Salisbury, "Playing It Safe," *IEEE Robotics and Automation Magazine*, vol. 11, pp. 12-21, 2004.

[6] J. Newman, "Head injury criteria in automotive crash testing," presented at 24th Stapp Car Crash Conference, 1980.

[7] G. A. Pratt and M. M. Williamson, "Series Elastic Actuators," presented at International Conference on Robotic Systems (IROS), 1995.

[8] M. M. Williamson, "Series Elastic Actuators," in *Department of Electrical Engineering and Computer Science*. Boston: Massachusetts Institute of Technology, 1995.

[9] D. W. Robinson, "Design and Analysis of Series Elasticity in Closed-loop Actuator Force Control," in *Department of Mechanical Engineering*: Massachusetts Institute of Technology, 2000.

[10] G. Tonietti, R. Schiavi, and A. Bicchi, "Design and Control of a Variable Stiffness Actuator for Safe and Fast Physical Human/Robot Interaction," in *International Conference on Robotics and Automation*. Barcelona, Spain: IEEE, 2005.